

図・本館

Cross-Field Electron Heat Transport  
due to High Frequency Electrostatic Waves

Hiroshi NAITOU

Institute of Plasma Physics,  
Nagoya University, Nagoya 464

[Received July 20, 1979]

Cross-field electron heat diffusion due to thermally excited high frequency electrostatic waves propagating almost perpendicular to the magnetic field is studied using a 2-1/2-dimensional simulation code. It is shown that the electron heat diffusion coefficient  $D_H$  is an order of magnitude greater than the electron particle diffusion coefficient  $D_p$ , which is essentially collisional. The characteristic feature of wave transport is observed, namely an increase of  $D_H$  with increasing values of the characteristic temperature scale length  $L_x$ . The heat diffusion coefficients  $D_H^{\parallel}$  and  $D_H^{\perp}$  for the parallel and perpendicular temperatures ( $D_H \approx D_H^{\parallel} + D_H^{\perp}$ ) show quite different magnetic field scalings since  $D_H^{\parallel}$  is due to ion modes while  $D_H^{\perp}$  arises from electron modes. This is also confirmed by treating the ions as an immobile background.

## §1. Introduction

Particle simulation has helped to clarify the basic physics responsible for the anomalous plasma and heat transport across a magnetic field.<sup>1-3)</sup> In particular, it has been shown<sup>1,3)</sup> that, even in a plasma quite near thermal equilibrium, cross-field transport coefficients can be an order of magnitude greater than the classical collisional ones.<sup>4)</sup> Even within the electrostatic approximation for the self-consistent electric fields in the plasma, this enhanced transport can arise from various mechanisms. One example is the low frequency convective cells<sup>5,6)</sup> and the other, which we treat in this work, is a random walk of high frequency waves.<sup>7,8)</sup> These waves propagate freely across the magnetic field, unlike the charged particles, carrying wave energy. A net energy flux results if there is a temperature gradient, since the spontaneous emission and absorption of the waves depend on the local temperature.

Generally the magnetic field scaling of the cross-field heat diffusion coefficient  $D_H$  is not same as that of the cross-field particle diffusion coefficient  $D_p$ , in contrast to classical collisional theory.<sup>4)</sup> It has been shown<sup>9)</sup> that  $D_H$  can be considerably smaller than  $D_p$  for the convective cell transport. In an actual plasma, energy transport by high frequency waves also contributes to  $D_H$ . If magnetic shear is introduced, convective transport is reduced to a collisional level<sup>10)</sup>; in that case  $D_H$  can be an order of magnitude greater than  $D_p$  because the wave energy transport only enhances the heat diffusion. Although this wave energy transport process

has been investigated extensively only for plasma waves<sup>7,8)</sup> and ion acoustic waves,<sup>7)</sup> other waves can also have an important effect on plasma confinement.

This paper reports a computer simulation study of heat diffusion in a plasma near thermal equilibrium due to electrostatic high frequency waves propagating nearly perpendicular to the magnetic field. These waves can exhibit Landau or cyclotron damping although the damping rate  $\gamma$  is quite small. Since the mean free path  $\ell_{\text{mfp}}$  is very large for small  $\gamma$ , these modes can cause large heat diffusion if the characteristic length  $L_x$  of the temperature variation is sufficiently large ( $L_x > \ell_{\text{mfp}}$ ). Thus  $D_H$  should be an increasing function of  $L_x$ ; indeed this is a characteristic feature of heat diffusion due to wave transport. Because of the nature of the collisionless damping, electron modes ( $\omega \gtrsim \omega_{ce}$ , where  $\omega_{ce}$  is the electron cyclotron frequency) should cause relaxation of the perpendicular temperature ( $T_{\perp}$ ) through cyclotron damping, while ion modes ( $\omega < \omega_{ce}$ ) should give rise to diffusion of the parallel temperature ( $T_{\parallel}$ ) through Landau damping. Since the diffusion of  $T_{\parallel}$  and  $T_{\perp}$  corresponds to heat diffusion coefficients,  $D_H^{\parallel}$  and  $D_H^{\perp}$ , respectively, we can separate the effects of ion and electron modes by observing these two coefficients. We can further confirm this by making the ions an immobile background. A careful investigation of the magnetic field scalings for these coefficients leads to the result that  $D_H^{\parallel}$  increases with the magnetic field while  $D_H^{\perp}$  decreases. Hence ion modes can significantly enhance the heat diffusion in a strong magnetic field ( $\omega_{ce}/\omega_{pe} \gtrsim 1$ ) where  $D_H^{\parallel}$  dominates over  $D_H^{\perp}$ .

Section 2 describes a simple theory of the electron heat diffusion due to high frequency waves. The treatment is essentially the same as that of Rosenbluth and Liu,<sup>7)</sup> but a more general expression for  $D_H$  is obtained. Section 3 shows the simulation results for  $D_p$ ,  $D_H$ ,  $D_H''$ , and  $D_H^\perp$ . Concluding remarks and discussions are given in §4.

## §2. Theory

Consider an infinite slab plasma in a uniform magnetic field  $\vec{B} = (0, B \sin\theta, B \cos\theta)$  ( $\theta$  is an arbitrary angle) with a nonuniform, periodic electron temperature and a constant ion temperature,

$$T_e(x) = T_0 [1 - \epsilon_T \cos(2\pi x/L_x)] \quad ; \quad T_i(x) = T_0 \quad . \quad (1)$$

Electron and ion densities are taken to be uniform ( $n_e = n_i = n_0$ ) and only electrostatic fluctuations in thermal equilibrium are considered. We will derive an analytical expression for  $D_H$  due to energy transport by high frequency waves in order to understand the general characteristics of wave transport phenomena.

The transport equation for the electrostatic wave energy per mode, with the wave number  $\vec{k}$ ,  $\epsilon_k = (\omega \frac{\partial \text{Re} \epsilon}{\partial \omega})_{\omega_k} \langle E_k^2 \rangle / 8\pi$  (where  $\epsilon$  is the dielectric function), may be written as<sup>7)</sup>

$$\frac{\partial \epsilon_k}{\partial t} + v_x \frac{\partial \epsilon_k}{\partial x} = 2\gamma_e T_e + 2\gamma_i T_i - 2\gamma \epsilon_k \quad (2)$$

where  $v_x$  and  $\omega_k$  are the group velocity in the x direction

and the frequency of a given mode, respectively;  $\gamma_e$  and  $\gamma_i$  are the spontaneous wave emission rates due to electron and ion thermal motions; and  $\gamma$  is the damping rate of the wave. Here it is assumed that  $L_x$  is much larger than the wavelength. For complete thermal equilibrium,  $T_e=T_i=T_0$ , we have  $\epsilon_k = T_0$  and  $\gamma = \gamma_e + \gamma_i$ . Following Rosenbluth and Liu<sup>7)</sup> the steady state solution of eq.(2) is given by

$$\epsilon_k(x) = \int_0^{\infty} d\mu \left[ \frac{\gamma_e}{\gamma} T_e(x') + \frac{\gamma_i}{\gamma} T_i(x') \right] e^{-\mu}, \quad (3)$$

where  $\mu$  represents the total convective damping of the given mode when it propagates from  $x'$  to  $x$  ;

$$\mu = \int_{x'}^x \frac{2\gamma}{v_x} dx'' \approx \frac{x-x'}{\ell_{\text{mfp}}} \text{sgn}(v_x), \quad (4)$$

and  $\ell_{\text{mfp}} = |v_x|/2\gamma$ . In eq.(4) we have used the assumption that wave properties are not affected by the temperature gradient ( $\epsilon_T \ll 1$ ). For the temperature profiles given by eq.(1), we can easily carry out the integration with respect to  $\mu$  in eq.(3):

$$\epsilon_k(x) = \frac{\gamma_e}{\gamma} T_0 \left[ 1 - \frac{\epsilon_T}{1+(2\pi\ell_{\text{mfp}}/L_x)^2} \cos \frac{2\pi x}{L_x} \right] + \frac{\gamma_i}{\gamma} T_0, \quad (5)$$

where we have used the fact that for  $x' < x$  only the wave propagating in the positive  $x$  direction contributes to  $\epsilon_k(x)$ , and for  $x' > x$  vice versa. The rate of increase of the thermal energy density of electrons at  $x$  is given by

$$\frac{3}{2} n_0 \frac{\partial T_e}{\partial t} = \sum_k [\gamma \epsilon_k(x) - \gamma_e T_e - \gamma_i T_i] \quad , \quad (6)$$

since, in steady state, this is just equal to the rate of decrease of the wave energy at  $x$ . Using eqs.(1) and (5), we can write eq.(6) as a diffusion type equation,

$$\frac{3}{2} n_0 \frac{\partial T_e}{\partial t} = n_0 D_H \frac{\partial^2 T_e}{\partial x^2} \quad , \quad (7)$$

where  $D_H$  is given by

$$n_0 D_H = \sum_k \frac{\gamma_e}{\gamma} \frac{v_x^2}{2\gamma} \frac{1}{1 + (2\pi \ell_{\text{mfp}}/L_x)^2} \quad . \quad (8)$$

We can interpret eq.(8) as follows. The factor  $\gamma_e/\gamma$  indicates that only the emission and damping of waves due to the electron thermal motion can cause electron heat diffusion; a similar expression involving  $\gamma_i/\gamma$  describes ion heat diffusion if there is a sinusoidal ion temperature variation. The factor  $v_x^2/2\gamma$  ( $=\ell_{\text{mfp}}^2/2\gamma$ ) is equal to the estimate coming from a simple random walk theory<sup>11)</sup> of wave energy transport. The last factor,  $[1 + (2\pi \ell_{\text{mfp}}/L_x)^2]^{-1}$ , includes the effects of the finite scale length of the temperature perturbation. When the coherence length of the mode is less than the scale length ( $\ell_{\text{mfp}} < L_x/2\pi$ ), this factor is very nearly unity and the random walk theory gives a good estimate. On the other hand when  $\ell_{\text{mfp}} > L_x/2\pi$ , the random walk approximation is not appropriate. This factor decreases with increasing  $\ell_{\text{mfp}}/L_x$  so

that waves having  $\ell_{\text{mfp}} \gg L_x/2\pi$  do not appreciably affect the heat diffusion.

The coefficient  $D_H$  can also be written in the form

$$n_0 D_H = \frac{L_x}{2\pi} \sum_k \frac{\gamma_e}{\gamma} v_x \frac{2\pi \ell_{\text{mfp}}/L_x}{1+(2\pi \ell_{\text{mfp}}/L_x)^2} \quad (9)$$

For a collisionless plasma,  $\ell_{\text{mfp}}$  can take arbitrary large values since for waves propagating almost perpendicular to the magnetic field  $\gamma \approx 0$ . However, for fixed  $L_x$  the last factor in eq.(9) takes on its maximum value, namely 1/2, for modes which have  $\ell_{\text{mfp}} = L_x/2\pi$ . Replacing this factor by 1/2 we have approximately

$$n_0 D_H \approx \frac{L_x}{4\pi} \sum_k \frac{\gamma_e}{\gamma} v_x \quad (10)$$

For two dimensional fluctuations in the x-y plane, which we simulate in the following section, we have the estimate for  $D_H$ , after replacing the summation over k by the integral in eq.(10);

$$D_H \approx \frac{L_x \langle v_x \rangle}{16\pi^2 n_0 \lambda_{De}^2} \quad (11)$$

where  $\langle v_x \rangle$  indicates the characteristic group velocity,  $\lambda_{De}$  is the electron Debye length, and we have assumed  $\gamma \approx \gamma_e$ . From eqs.(9)-(11) we see that  $D_H$  is approximately proportional to  $L_x$  for a collisionless plasma. This is the most characteristic feature of heat diffusion due to wave transport as first pointed out by Rosenbluth and Liu<sup>7)</sup> for plasma waves. (Note

that if the damping rate  $\gamma$  is not large enough to allow  $\lambda_{\text{mfp}} \lesssim L_x/2\pi$ ,  $D_H$  is smaller than the estimates given by eqs.(10) or (11).) Another characteristic feature of  $D_H$  which is apparent from eq.(11) is that  $D_H$  increases with the group velocity  $\langle v_x \rangle$ . These characteristic features of  $D_H$  will be investigated in the next section.

### §3. Simulation results

We present here the simulation results for electron heat diffusion. The model we used is a conventional 2-1/2-dimensional  $(x, y, v_x, v_y, v_z)$  electrostatic subtracted dipole expansion code (SUDS)<sup>12)</sup> with a uniform magnetic field  $\vec{B} = (0, B \sin\theta, B \cos\theta)$ . All physical quantities are assumed to be uniform in the  $z$  direction and the full Lorentz force is used to advance the particles. The angle  $\theta$  was set equal to  $10^\circ$  in all runs, so the angle between  $\vec{k}$  and  $\vec{B}$  can vary between  $80^\circ$  and  $90^\circ$ . Periodic boundary conditions are used in both the  $x$  and  $y$  directions, with the periods  $L_x$  and  $L_y$ .

Two sets of runs were made. One is for mobile ions,  $m_i/m_e = 100$ . The other is the case of immobile ions ( $m_i/m_e \rightarrow \infty$ ) where ions are assumed to be a charge neutralizing uniform background. An initial electron temperature given by eq.(1) with  $\epsilon = 0.2$  is used for both cases. Initially, electron guiding centers are positioned in a slightly nonuniform way in order to make the actual density uniform.<sup>13)</sup> For the case of mobile ions, the initial ion temperature is taken to be  $T_0$  and actual ion positions are distributed uniformly on the  $x$ - $y$  plane.



Test particle diffusion coefficients in the x and y' directions were measured in order to check the effects of convective and collisional transport (where y' is perpendicular to the magnetic field and the x-axis). They are determined from the temporal behavior of the mean squares displacements of the guiding centers from the initial positions;  $D_{px}^e = \lim_{t \rightarrow \infty} \langle \Delta x_g^2 \rangle / t$ ;  $D_{py'}^e = \lim_{t \rightarrow \infty} \langle \Delta y_g^2 \rangle / t \cos^2 \theta$ , etc.

The electron heat diffusion coefficients are measured in the following way. First, the time series of the most dominant Fourier modes of the electron temperatures,  $T_{AV}$ ,  $T_{\parallel}$ , and  $T_{\perp}$  ( $k_x = 2\pi/L_x$ ,  $k_y = 0$ , cosine component) are followed. Let  $T_{\parallel}$  and  $T_{\perp}$  be the parallel and perpendicular temperatures, and  $T_{AV}$  the average temperature:  $T_{\perp} = 1/2 \langle 1/2 m v_{\perp}^2 \rangle$ ,  $T_{\parallel} = \langle 1/2 m v_{\parallel}^2 \rangle$ , and  $T_{AV} = 1/3 (2T_{\perp} + T_{\parallel})$ . Assuming that the temperature evolves according to a diffusion type equation (cf. eq.(7)), we have the coefficients,

$$D_H = \frac{3}{2} \left( \frac{2\pi}{L_x} \right)^2 \frac{\partial}{\partial t} \ln T_{AV} \quad ; \quad (12a)$$

$$D_H^{\parallel} = \frac{1}{2} \left( \frac{2\pi}{L_x} \right)^2 \frac{\partial}{\partial t} \ln T_{\parallel} \quad ; \quad D_H^{\perp} = \left( \frac{2\pi}{L_x} \right)^2 \frac{\partial}{\partial t} \ln T_{\perp} \quad . \quad (12b)$$

Using eqs.(12), we obtain immediately

$$D_H \approx D_H^{\parallel} + D_H^{\perp} \quad , \quad (13)$$

since initially  $T_{AV} = T_{\parallel} = T_{\perp}$  and the temperatures do not differ greatly during the simulation time.

### 3.1 The case of mobile ions

Here we will discuss the case where the dynamics of both electrons and ions are followed. The parameters we used are:  $L_x=64, 128, 256, 512$ ;  $L_y=64$ ;  $\omega_{ce}/\omega_{pe}=2, 1, 1/2, 1/4, 1/8$ ; mass ratio,  $m_i/m_e=100$ ;  $\lambda_{De}=1$ ; number of electrons or ions per Debye square,  $n_0\lambda_{De}^2=1$ ; finite time step  $\Delta t=0.2$ ; total simulation time  $t_{END}=1000$ ; half width of a Gaussian cloud,  $a=1$ . All lengths and times are normalized by the unit size of the spatial grid,  $\Delta$ , and  $\omega_{pe}^{-1}$ . For these parameters the various collision frequencies are given by<sup>14)</sup>:  $\nu_{ee} \approx \nu_{ei} \approx 5 \times 10^{-3}$ ;  $\nu^e \approx (m_e/m_i)\nu_{ei} \approx 5 \times 10^{-5}$ ;  $\nu_{eT} \approx \sin\theta \nu_{ei} \approx 10^{-3}$ , where  $\nu_{ee}$  and  $\nu_{ei}$  are the electron-electron and electron-ion collision frequencies;  $\nu^e$  is the collision frequency for thermal equilibrium between electrons and ions;  $\nu_{eT}$  is the collision frequency for electron temperature anisotropy. (The estimate for  $\nu_{eT}$  comes from the special character of the 2-1/2-D model in which only the projection of particle parallel motion on the x-y plane are simulated.) Therefore, we can neglect the collisional process for thermal equilibrium between electrons and ions and for temperature anisotropy during the simulation time.

Figure 1 represents the measurements for  $D_{px}^e$ ,  $D_{py}^e$ ,  $D_{px}^i$  and  $D_{py}^i$ , averaged over runs with various values of  $L_x$  varying from 64 to 512. The measured diffusion coefficients showed no appreciable dependence on  $L_x$ . The solid lines in the figure represent the classical collisional dependence ( $B^{-2}$ ) of particle diffusion for ions (upper line) and electrons (lower line). The observed  $D_{px}^e$  is almost collisional although a

slight enhancement is detected for the stronger magnetic fields. The coefficients,  $D_{py}^e$ ,  $D_{px}^i$ , and  $D_{py}^i$ , give larger enhancements over the collisional levels as the magnetic field increases due to the low frequency fluctuations. However these enhancements are much smaller than in the pure 2-D case since the electron motions along the field lines effectively short out the fluctuations. Electrons moving along the B-field, feel an averaged  $E_y$  field because of their faster speed<sup>6)</sup> and therefore have less motion in the x direction due to the  $cE_y/B$  drift. Hence  $D_{px}^e$  is almost collisional and we can presume that  $D_H$  should be the order of  $D_{px}^e$  if there were no other anomalous transport.

The examples of the time behaviors of the most dominant Fourier modes of the electron temperatures are presented in Fig. 2. The straight lines in the figures are drawn using a least squares method and the coefficients,  $D_H$ ,  $D_H''$ , and  $D_H^\perp$ , are obtained from the slopes of these lines. Figure 2(a) indicates the rather strong magnetic field case,  $\omega_{ce}/\omega_{pe} = 1$  and  $L_x = 256$ . We can see that the relaxation of the parallel temperature is considerably faster than that of the perpendicular temperature. In this case, classical collisional transport is quite small due to the rather strong magnetic field. Note that, in the collisionless system, the relaxation of  $T_{\parallel}$  comes from the electron Landau damping (or emission) of the waves<sup>8)</sup> and that the relaxation of  $T_{\perp}$  comes mainly from the electron cyclotron damping. The electron Landau damping occurs dominantly for the ion modes ( $\omega < \omega_{ce}$ , i.e., the lower hybrid mode, electrostatic ion cyclotron mode, and ion Bernstein

modes) whereas the electron cyclotron damping comes mainly from the electron modes ( $\omega \gtrsim \omega_{ce}$ , i.e., upper hybrid mode and electron Bernstein modes). Ion Landau and ion cyclotron damping do not influence the relaxation of the electron temperature except through the propagation properties, as discussed in §2. We can see clearly from Fig. 2(a) that the heat transport due to ion modes is predominant over that due to electron modes in the strong magnetic field case. The relaxation of  $T_{AV}$  is intermediate between the relaxation of  $T_{\parallel}$  and  $T_{\perp}$ . Figure 2(b) shows the weakest magnetic field case,  $\omega_{ce}/\omega_{pe} = 1/8$  and  $L_x = 256$ . The relaxation of  $T_{\perp}$  is faster than  $T_{\parallel}$  in contrast to the strong magnetic field case. In this case classical heat diffusion is dominant because of its  $B^{-2}$  dependence. For the collisional diffusion  $T_{\perp}$  should relax approximately twice as fast as  $T_{\parallel}$ , which agrees very well with the simulation results. (This estimate is obtained under the assumption that the relaxation of  $T_{\parallel}$  is only caused by the transport of the parallel kinetic energy associated with the particle diffusion in the x direction; in fact, if  $D_H^{\perp} \approx D_C$  where  $D_C$  is the collisional particle diffusion coefficient,  $D_H^{\parallel} \approx 1/4 D_C$  and  $D_H^{\perp} \approx 5/4 D_C$ .)

The magnetic field scaling of  $D_H$  for various  $L_x$  are shown in Fig. 3. The solid line shows the collisional law for the heat diffusion, whose value is almost same as  $D_{px}^e$  in Fig. 1. We see that the magnetic field scaling of  $D_H$  for a fixed  $L_x$  is considerably different from the collisional one and that the measured  $D_H$  values are an order of magnitude greater than the collisional case except for the weakest magnetic field case.

This enhancement of  $D_H$  above the collisional level must come from the wave energy transport of high frequency modes. The most characteristic feature of  $D_H$  due to wave transport is its  $L_x$  dependence. Figure 3 shows that as  $L_x$  increases,  $D_H$  also increases, approximately in proportion to  $L_x$ , which agrees well with the estimate in §2. This  $L_x$  dependence is quite different from the collisional or convective diffusion.

Figure 4(a) indicates the magnetic field scaling of  $D_H''$ . Again  $D_H''$  increases approximately in proportion to  $L_x$ ; this is clearer for the stronger magnetic field cases. As the magnetic field increases  $D_H''$  also increases, except for the weakest magnetic field case, with  $L_x$  fixed. The increasing slope of  $D_H''$  for the weakest magnetic field arises mainly from the classical collisional process, which is of the order of  $1/4 D_c$ . The reason why  $D_H''$  increases with the magnetic field can be explained in the following way. As we have discussed previously, the enhancement of  $D_H''$  from the collisional level is caused by the wave transport of ion modes through electron Landau damping and its inverse process. When the magnetic field is sufficiently strong ( $\omega_{ce}/\omega_{pe} > 1$ ), Landau damping occurs due to the electron parallel motion to the magnetic field. However when the magnetic field becomes weaker ( $\omega_{ce}/\omega_{pe} < 1$ ), the Landau damping rate is reduced considerably because, for  $k_{\perp}^2 \rho_e^2 > 1$  modes, the Larmor motion of a particle around the field line can average out the electric field that the particle sees (finite Larmor radius effect). Thus the step size of the random walk becomes larger as the magnetic field gets weaker. If  $L_x$  is fixed,  $\lambda_{mfp}$  for the mode becomes greater than  $L_x/2\pi$  and that mode can not

contribute to  $D_H''$  effectively; hence  $D_H''$  decrease for  $\omega_{ce}/\omega_{pe} < 1$ .

Figure 4(b) shows the measurements for  $D_H^\perp$ . The enhancement over the collisional law is apparent. The magnetic field scaling for  $D_H^\perp$  is considerably different from that for  $D_H''$ . The coefficient  $D_H^\perp$  decreases as the magnetic field increases. Again  $D_H^\perp$  is roughly in proportion to  $L_x$  although its dependence is not so clear as for  $D_H''$ . This magnetic field scaling of  $D_H^\perp$  arises because the group velocity of the electron modes becomes small as the magnetic field increases (see eq.(11)). The summation of  $D_H^\perp$  and  $D_H''$  is almost  $D_H$  as is consistent with eq.(13).

### 3.2 The Case of Immobile Ions

We have shown that the effects of ion and electron modes are clearly identified in the measurements for  $D_H''$  and  $D_H^\perp$ , respectively. To confirm this result, additional set of runs were conducted where ions are assumed to form an immobile, constant background. The parameters we used are:  $L_x = 256$ ;  $L_y = 128$ ;  $\omega_{ce}/\omega_{pe} = 2-1/7$ ;  $\lambda_{De} = 1$ ;  $a = 1$ ;  $n_0 \lambda_{De}^2 = 1$ ;  $\Delta t = 0.2$ ;  $t_{END} = 1000$ .

The measurement for  $D_{px}^e$  and  $D_{py}^e$  are presented in Fig.5. The dependence of  $D_{px}^e$  on the magnetic field strength agrees very well with the collisional theory ( $D_c$ ) using an empirically determined factor associated with the use of finite size particles.<sup>9)</sup> The magnetic field scaling for  $D_{py}^e$ , is that of the convective mode. From this observation we can expect that the collisional part of  $D_H$  should be nearly equal to  $D_{px}^e \approx D_c$ .

Figure 6 indicates the magnetic field scalings of  $D_H'$ ,

$D_H''$ , and  $D_H^\perp$ . The solid lines represent the collisional  $D_H$  ( $\approx 5/4 D_C$ ) and  $D_H''$  ( $\approx 1/4 D_C$ ). For  $\omega_{ce}/\omega_{pe} < 1/2$  the measured points are almost collisional while for  $\omega_{ce}/\omega_{pe} > 1/2$  an enhancement of the heat diffusion coefficients from the collisional law is observed. The important result is that  $D_H^\perp$  is almost the same as  $D_H$  while  $D_H''$  is considerably smaller than  $D_H^\perp$ . This is because ion modes are not included in this case. A dramatic difference in  $D_H''$  is observed for the cases of mobile and immobile ions (Fig. 4(a) and 6); this confirms that ion modes contribute mainly to the enhancement of  $D_H''$ . On the other hand no drastic change is observed for  $D_H^\perp$ ; this verifies that electron modes contribute largely to  $D_H^\perp$ . Because the collisional damping of electron modes due to electron-ion collision arises in the case of mobile ions, the magnetic field scalings for  $D_H^\perp$  differ slightly for the mobile and immobile ion cases; i.e.,  $D_H^\perp$  is larger than the collisional level even for the weaker magnetic field for the mobile ion case, while  $D_H^\perp$  is almost  $D_C$  for the immobile ion case.

#### §4. Discussions and Conclusions

We have obtained the heat diffusion coefficients of electrons experimentally by observing the temporal and spatial variations of a sinusoidal temperature perturbation superposed on a constant temperature in the 2-1/2-D plasma model. In this model, convective cell transport is eliminated naturally and the particle diffusion measurement confirms the classical collisional dependence. We have shown in §2 that  $D_H$  can be

obtained analytically in the form quite similar to the random walk theory but including the effect of the temperature scale length  $L_x$ . If the mean free path,  $\ell_{\text{mfp}}$ , of the mode is considerably larger than  $L_x/2\pi$ , the mode cannot contribute to  $D_H$ ; otherwise the mode can enhance  $D_H$ . Then  $D_H$  becomes an increasing function of  $L_x$  because larger  $\ell_{\text{mfp}}$  waves contribute to  $D_H$  for larger  $L_x$ . Simulation results show that  $D_H$  is roughly in proportion to  $L_x$  and is considerably larger than  $D_{\text{px}}^e (\approx D_c)$ . We have also measured  $D_H''$  and  $D_H^\perp$  from the relaxation of the parallel and perpendicular temperatures. For the collisionless system Landau damping (or its inverse process) mainly contribute to  $T_{\parallel}$  damping whereas cyclotron damping contributes to  $T_{\perp}$  damping. Landau damping comes from ion modes (lower hybrid mode, electrostatic ion cyclotron mode, and ion Bernstein modes) while cyclotron damping comes from electron modes (upper hybrid and electron Bernstein modes). In our system, collisional damping for the  $v_{\parallel}$  motion is considerably less than for the  $v_{\perp}$  motion. Hence  $T_{\parallel}$  damping mainly comes from the collisionless Landau damping while  $T_{\perp}$  damping is caused by the cyclotron and collisional damping. Simulation results show clearly the separation between  $D_H''$  and  $D_H^\perp$ .  $D_H''$  is an increasing function of the magnetic field while  $D_H^\perp$  is a decreasing function of  $B$ . These results are consistent with the qualitative estimates and the phenomena have been further verified by eliminating the ion modes in the simulation, treating ions as the immobile background.

These simulation results, together with the simple



theoretical estimate, confirm the importance of contributions to  $D_H$  from wave energy transport by almost perpendicularly propagating waves. This transport mechanism is more significant for larger systems. Magnetic field scalings of  $D_H''$  and  $D_H^\perp$  indicate that ion modes are important in the stronger magnetic field system. This is quite significant, because these modes can be excited to amplitudes considerably above the thermal level as a consequence of plasma heating by lower hybrid waves, ion cyclotron waves, etc.

Although the magnetic field scaling of  $D_H$ ,  $D_H''$ , and  $D_H^\perp$  shows the characteristic features of the wave energy transport, their absolute magnitudes are not verified rigorously by the theory because there is no explicit expression of  $D_H$  for arbitrary waves and there are many wave modes in the magnetized plasma. The derivation of an explicit expression for  $D_H$  will be studied in the future but the resulting theoretical expression should be consistent with the characteristic features obtained in the present work.

#### Acknowledgements

The author wishes to express his thanks to Professor T. Kamimura for stimulating suggestions and discussions. He is also grateful to Professor Y. Terashima, Professor J.M. Dawson, and Professor B.D. Fried for their valuable discussions. Assistance with the computer simulations was provided by members of the computer center of the Institute of Plasma Physics.

## References

- 1) J.M. Dawson, H. Okuda and B. Rosen: in *Methods in Computational Physics*, ed. J. Killeen (Academic Press, New York, San Francisco, London, 1976) Vol.16, p.281.
- 2) C.Z. Cheng and H. Okuda: *Phys. Rev. Letters* 38(1977) 708.
- 3) A.T. Lin, J.M. Dawson and H. Okuda: *Phys. Rev. Letters* 41(1978) 753.
- 4) S.I. Braginskii: in *Reviews of Plasma Physics*, ed. M.A. Leontovich (Consultants Bureau, New York, 1965) Vol.1, p.205.
- 5) J.B. Taylor and B. McNamara: *Phys. of Fluids* 14(1971) 1492.
- 6) H. Okuda and J.M. Dawson: *Phys. of Fluids* 16(1973) 408.
- 7) M.N. Rosenbluth and C.S. Liu: *Phys. of Fluids* 19(1976) 815.
- 8) J. Canosa and H. Okuda: *Phys. of Fluids* 18(1975) 335.
- 9) H. Naitou, T. Kamimura and J.M. Dawson: *J. Phys. Soc. Japan* 46(1979) 258.
- 10) H. Okuda and J.M. Dawson: *Phys. of Fluids* 16(1973) 1456.
- 11) S. Chandrasekhar: *Rev. mod. Phys.* 15(1943) 1.
- 12) W.L. Kruer, J.M. Dawson and B. Rosen: *J. Comp. Phys.* 13(1973) 114.
- 13) H. Naitou, S. Tokuda and T. Kamimura: *Res. Note of Inst. Plasma Physics (Nagoya), IPPJ* 356 (September 1978).
- 14) Y. Matsuda and H. Okuda: *Phys. of Fluids* 18(1975) 1740.

## Figure Captions

- Fig.1. Magnetic field scaling of the particle diffusion coefficients for electrons and ions. The solid lines show the collisional dependence ( $\propto B^{-2}$ ).
- Fig.2. Examples of the temporal evolution of the most dominant Fourier modes of the temperatures for (a)  $\omega_{ce}/\omega_{pe} = 1$  and (b)  $\omega_{ce}/\omega_{pe} = 1/8$  with  $L_x = 256$ .
- Fig.3. Magnetic field scaling of  $D_H$  for different  $L_x$ .
- Fig.4. Magnetic field scaling of (a)  $D_H''$  and (b)  $D_H^\perp$  for different  $L_x$ .
- Fig.5. The particle diffusion coefficients versus magnetic field strength for the case of immobile ions.
- Fig.6. Magnetic field scaling of  $D_H$ ,  $D_H''$ , and  $D_H^\perp$  for the case of immobile ions.

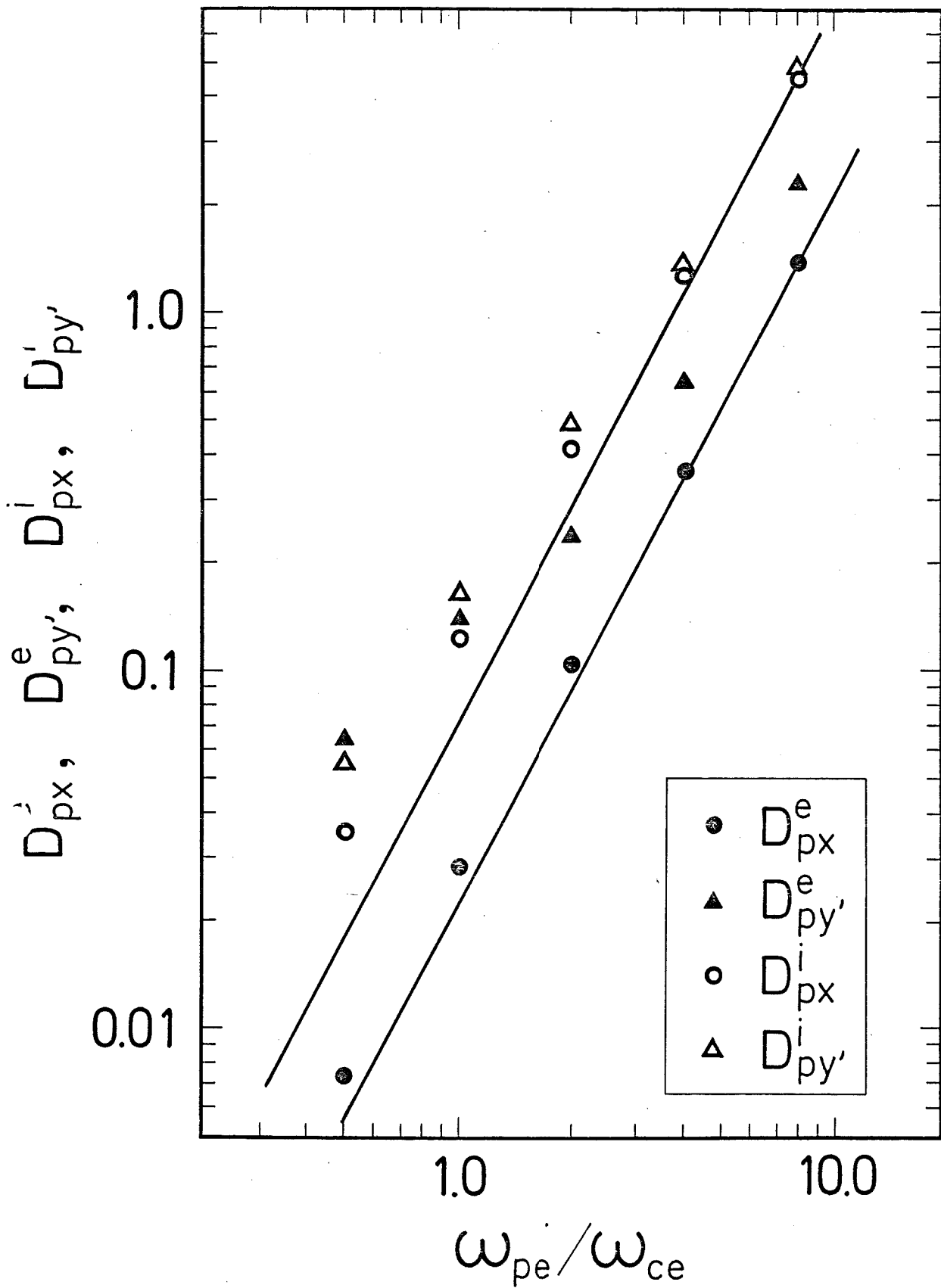


Fig. 1. H. Naitou

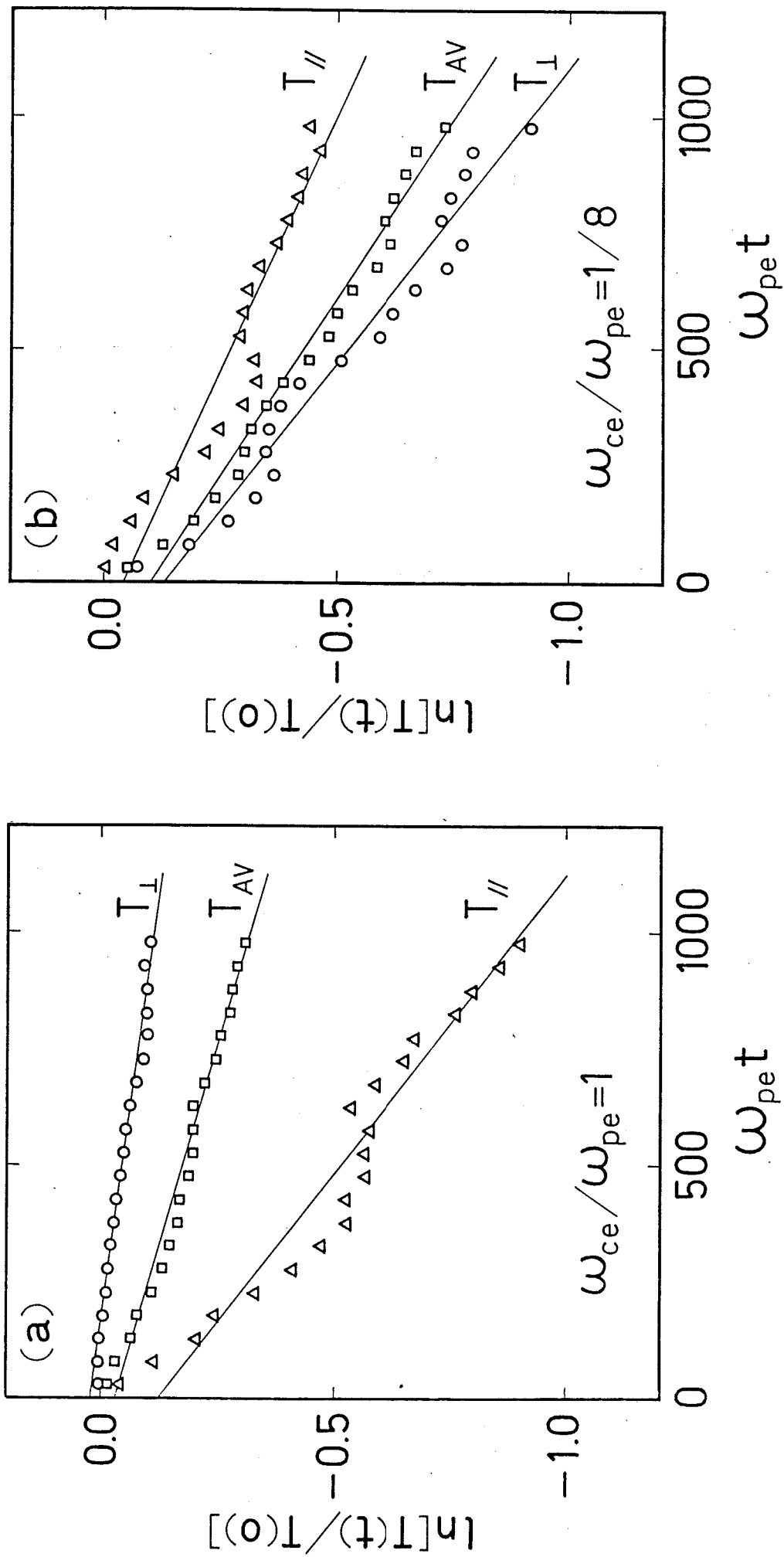


Fig. 2. H. Naitou

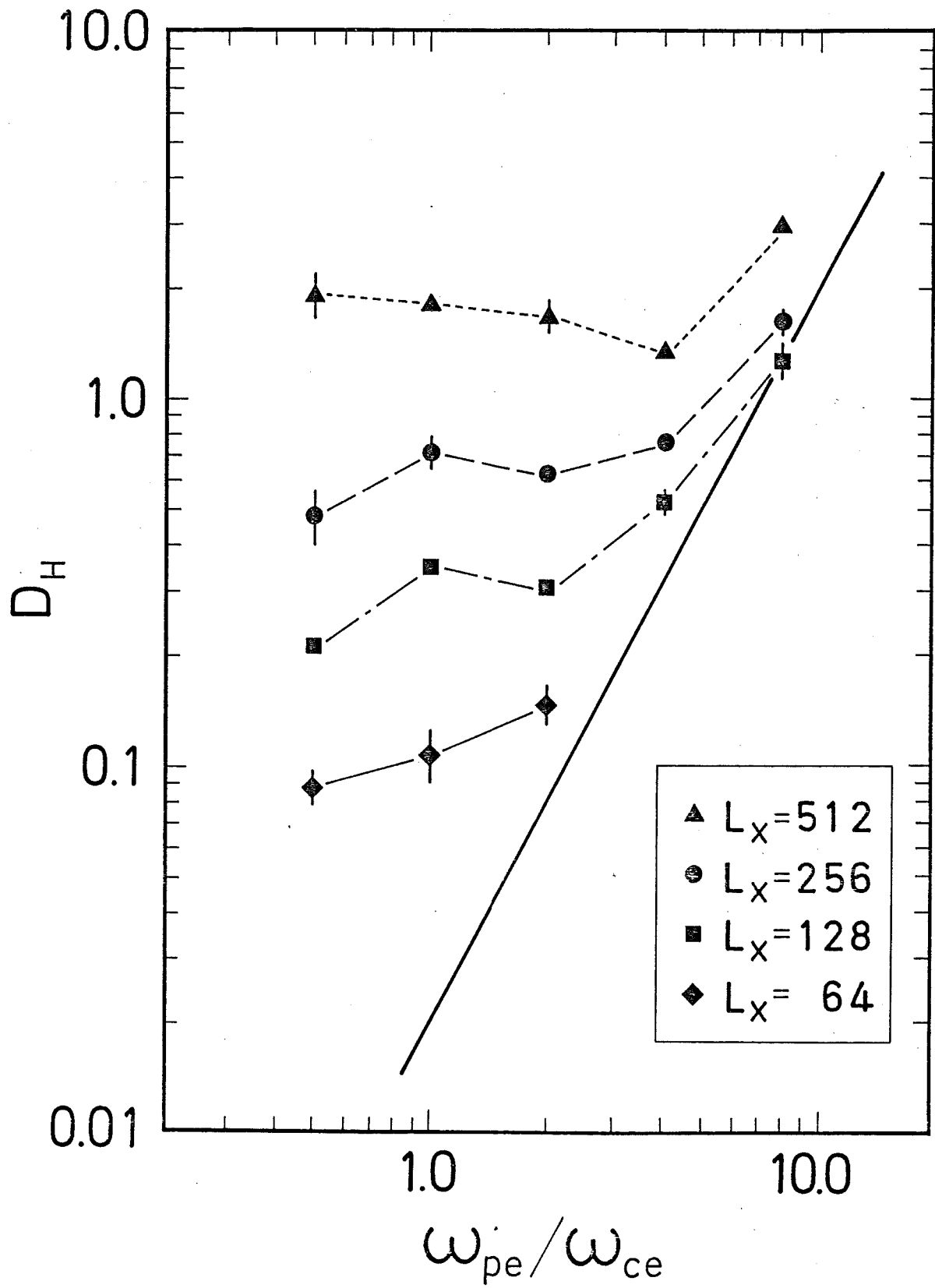


Fig. 3. H. Naitou

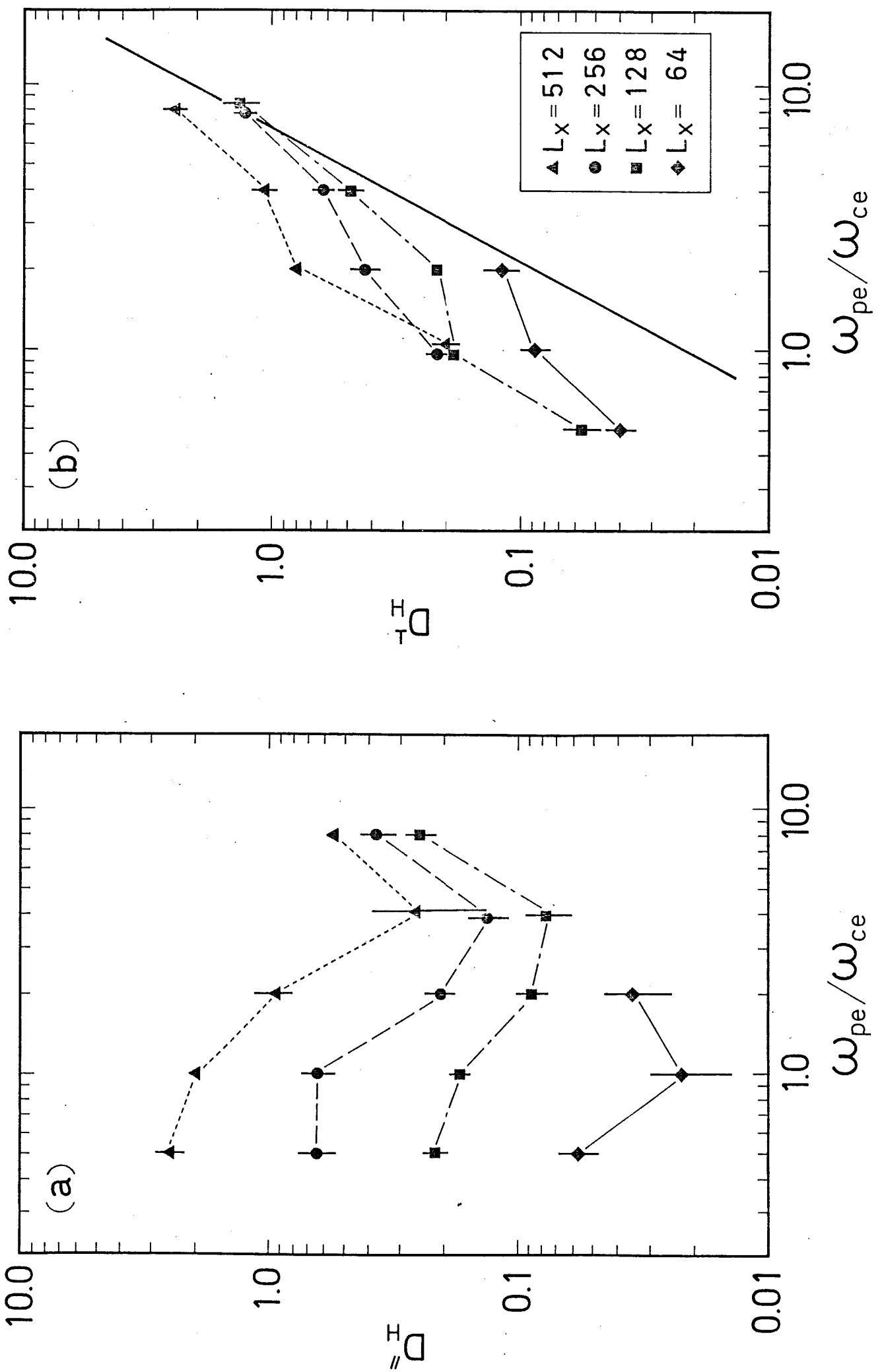


FIG. 4. H N I T O S . . .

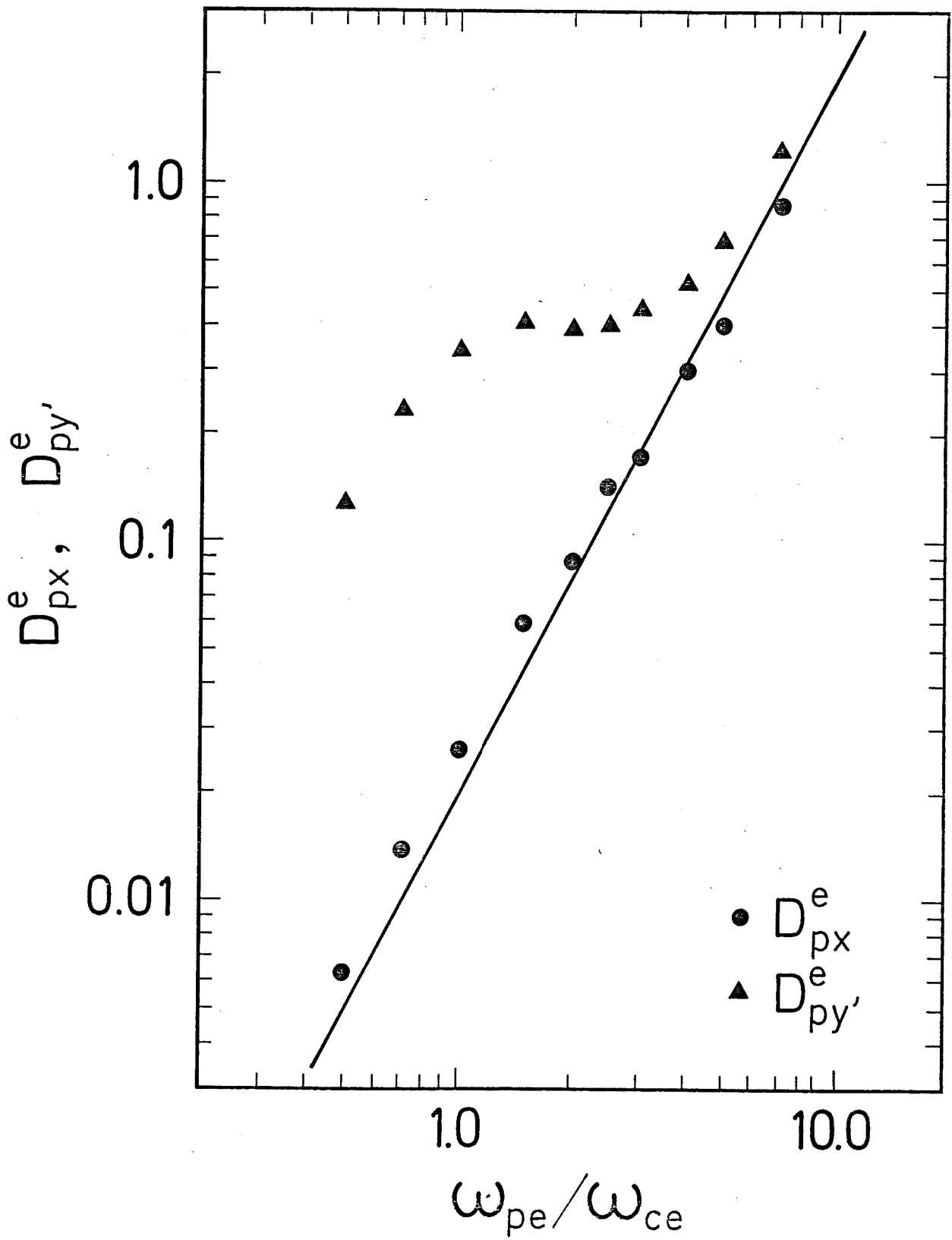


Fig. 5. H. Naitou



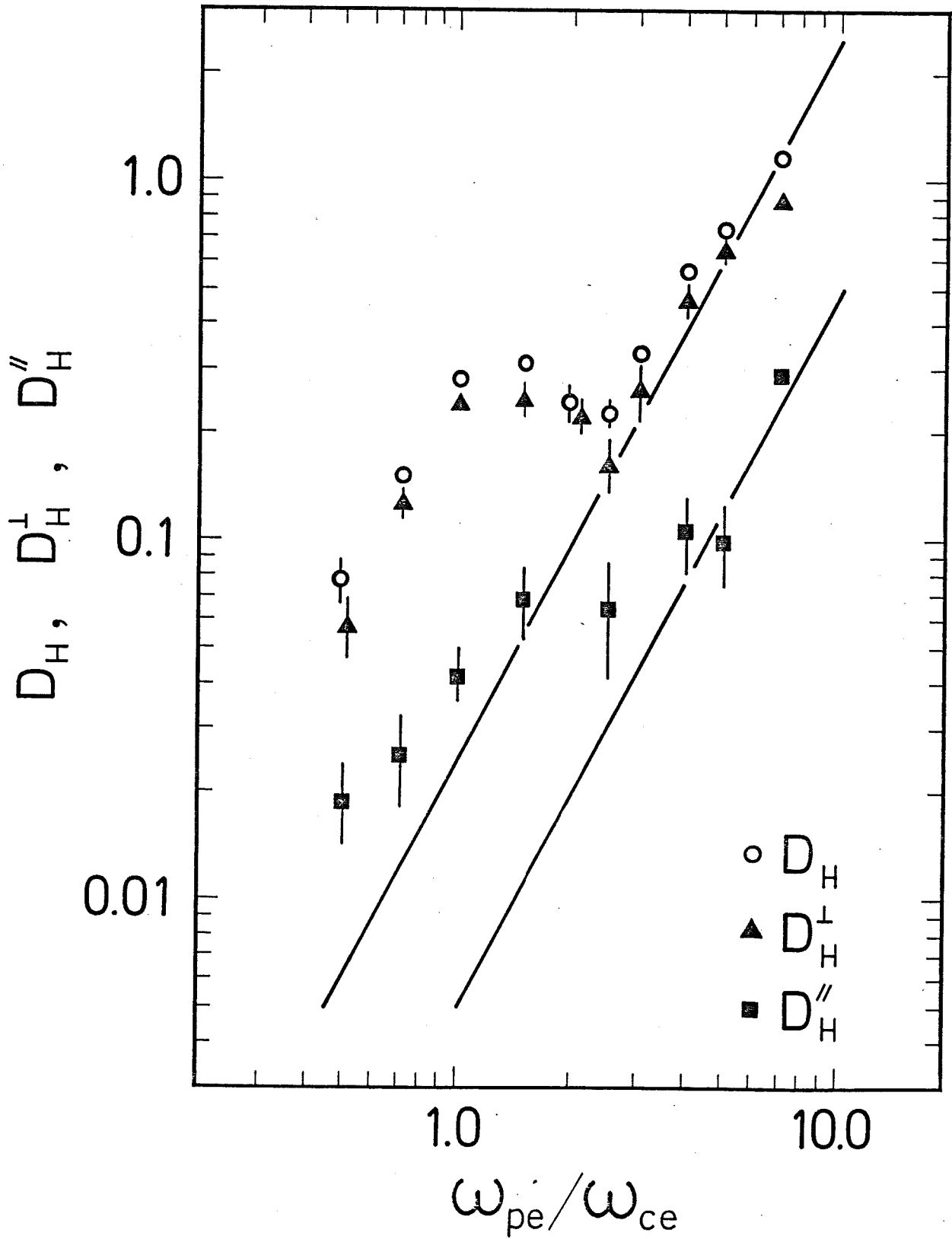


Fig. 6. H. Naitou